International Journal of Materials and Chemistry 2015, 5(2): 31-43
DOI: 10.5923/j.ijmc.20150502.02

Synthesis, Characterization and DFT Calculations of 1,4-diphenyl-3-(p-nitrophenylamino)-1,2,4-triazolium Hydroxide Inner Salt (Nitronitron) by ^{1}H NMR, FT-IR, UV/Vis and HOMO-LUMO Analysis

Zeyad A. Saleh[1], Firyal Weli Askar[2], Salah M. A. Ridha[3,*]

[1]Physics Department, College of Science, AL-Mustansiriyah University, Baghdad, Iraq
[2]Chemistry Department, College of Science, AL-Mustansiriyah University, Baghdad, Iraq
[3]Physics Department, College of Science, Kirkuk University, Kirkuk, Iraq

Abstract In this study, the synthesis and characterization of a novel compound, (1,4-Diphenyl-3- (p-nitrophenylamino) -1,2,4-triazolium hydroxide inner salt (Nitonitron), $C_{20}H_{15}N_5O_2$) were reported. The spectroscopic investigations of the compound were studied by 1H NMR, FT-IR, UV/Vis techniques. The 1H NMR spectra were recorded in DMSO solution. FT-IR spectrum in solid state was observed in the region 4000-400 cm^{-1}. The UV/Vis absorption spectrum of the compound which dissolved in chloroform was recorded in the range 200-800 nm. The structural data, fundamental vibrational modes, 1H NMR isotropic chemical shifts, frontier orbital energies (HOMO, LUMO), and band gap energy of the compound in the ground state were calculated using density functional theory(DFT) employing B3LYP/6-311G(d,p) basis set. The HOMO and LUMO analysis were used to elucidate information regarding charge transfer within the molecule. Based on the optimized geometry and by using time-dependent density functional theory (TD-DFT) methods in vacuum and solution (chloroform), the allowed excitation and oscillator strengths of electronic absorption spectrum were predicted. The solvation effects have been included by means of the conductor-like polarizable continuum model CPCM. Isotropic chemical shifts were calculated using the Gauge-Independent Atomic Orbital (GIOAO) method. Finally, a comparison between the experimental data and the calculated results appeared a good agreement.

Keywords Nitronitron, Heterocyclic compound, ^{1}H NMR, IR, UV/Vis, DFT

1. Introduction

A large number of heterocyclic compounds, nitrogen-containing heterocycles such as, 1,2,4-triazoles and its derivatives, are an important class of compounds which possess large variety of applications due to their broad-spectrum biological activities, such as antimicrobial [1-3], antibacterial [4, 5], anti-tumor [6], antihypertensive agents [7], antifungal [8-10], anticancer [11], inhibition of vitiligo disease [12], and antiviral [13]. Apart from its biological importance, the use triazole derivatives in the field of anticorrosion protection of metals and alloys [14]. in addition, in 2009, it was demonstrated that triazoles derivatives is used as photosensitizers for dye-sensitized solar cells [15]. To our knowledge, neither the experimental nor computational studies of the synthesized compound of Nitronitron have been available until now.

Considering the large physical, biological, and industrial significance, we synthesized Nitronitron based on Nitron by using nitration method. The aim of the present work is to analysis the results obtained from IR, UV/Vis and NMR spectra, and to calculate molecular structure parameters (bond lengths, bond angles, dihedral angles) and fundamental vibrational frequencies associated of Nitronitron compound (Scheme 1).

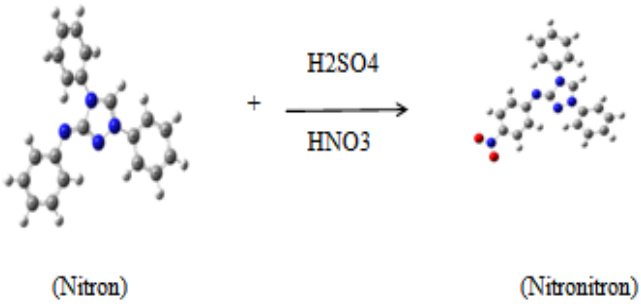

Scheme 1. Synthesis of Nitronitron

* Corresponding author:
salah_yagmuroglu@yahoo.com (Salah M. A. Ridha)
Published online at http://journal.sapub.org/ijmc

The theoretical calculations included the geometric parameters, HOMO and LUMO energies, absorption wavelengths, excitation energies, vibrational frequencies, and 1H NMR chemical shifts of synthesized molecule by using Gaussian 09 package [16]. The results obtained from theoretical calculations and experimental were compared.

2. Materials and Methods

2.1. Synthesis

A mixture of (4.2 ml, 0.087 mole) concentrated sulfuric acid and (9. 6 ml, 0.092mole) nitric acid was added drop by drop of (3.123 gm, 0.01 mole) of Nitron compound with continuous stirring in ice bath for a period of 2 hours, at 5Co. The reaction mixture was poured in to ice, the precipitate was filtered, dried then purified by column chromatography using silica gel eluting with petroleum ether(60-80)°C / benzene (1:1).

Yield: 75%.

Melting Point: 183-185°C.

Color: Yellow

FT-IR (KBr, ν, cm-1): 1537 (C=N), 1602(C=C), 1570, 1333(NO2).

UV–Vis (Chloroform): λ_{max} /nm (log ε) 430 (0.99).

1H NMR (300 MHz, DMSO-d6, δ, ppm): 8.775 (s, 1H, C_1-H), 8.690-8.663 (m,4H), 8.531-7.669 (m, 10H, Ar-H).

3. Experimental Details

3.1. FT-IR Spectrum

Fourier transform-infrared (FT-IR) measurements were carried out by the KBr method using a Shimadzu corporation 8400S FT-IR spectrometer. FT-IR spectra are generated by the absorption of electromagnetic radiation in the frequency range 4000–400 cm^{-1}.

3.2. UV–Vis Spectrum

UV/Vis spectrum of the compound has been recorded in the region of 200–800 nm using a Perkin Elmer Lambda 35 UV–Vis spectrometer.

3.3. ^{1}H NMR Spectrum

^{1}H NMR spectrum was recorded (299K) on AV300 MHz spectrometer. The compound was dissolved in DMSO. Chemical shifts were reported in ppm relative to tetramethylsilane (TMS) for 1H NMR. ^{1}H NMR spectrum was obtained at a base frequency of 300 MHz.

4. Computational Method

The molecular geometry, with no symmetry constrains, was optimized using density functional theory (DFT) calculations with a hybrid functional B3LYP (Becke's three parameter exchange functional combined with the LYP gradient corrected correlation functional) at the basis set 6-311G(d.p) by the Berny method [17] to characterized all stationary points as minima. The optimized geometry corresponding to the minimum on the potential energy surface (PES) has been obtained by solving self-consisting field equation iteratively. The calculated vibrational frequencies ascertained that the structure was stable (no imaginary frequency). TD-DFT method is usually found to be a strong and accurate method for describing low-lying excited states of conjugated molecules and has consequently been applied to solve countless chemical and physical problems. Based on the optimized geometry and by using time-dependent density functional theory (TD-DFT) methods in vacuum and solution (chloroform), the allowed excitation and oscillator strengths of electronic absorption spectrum were predicted. The solvation effects have been included by means of the conductor-like polarizable continuum model CPCM [18].

In addition, HOMO, LUMO, and energy gap of the title compound were calculated at the B3LYP/6-311G(d,p) level. Finally the Nuclear Magnetic Resonance (NMR) chemical shifts were performed using Gauge Independent Atomic Orbital (GIAO) method [19, 20].

5. Results and Discussion

5.1. Molecular Geometry

The most optimized structural parameters (bond lengths, bond angles and dihedral angles) of Nitronitron were calculated by DFT/B3LYP level with 6-311G(d,p) basis set and are given in Table 1. The calculated molecular structure of the title compound is found to be non-planar and is as shown in Figure 1. along with the atom numbering scheme. In the literature, we have not found experimental data on molecular structure of Nitronitron, therefore the molecular structure of Nitronitron is compared with the available experimental data ofN-(p-dimethylaminobenzylidene)-p-nitroaniline (DBN) and 5-[(E)-Methoxy(phenyl)methylidene]-1,3,4-triphenyl-4,5-dihydro-1H-1,2,4-triazole [21, 22] as crystal data of Nitronitron. As seen in Table 1, all of the bond lengths and bond angles in the phenyl rings are in the normal range. The calculated double N35=C1 and N37=C38 bond lengths were found as 1.3221 and 1.2953 Å, while the single N36-C1, N34-C38 bond lengths in 1,2,4 triazole ring are calculated as 1.3407 and 1.3539 Å, respectively. These single bonds are shorter than expected in triazole ring. This result indicates strong interaction of the filled nitrogen 2p orbital with unoccupied carbon 2p orbital. The calculated single C6-N37 and C3-N40 bond lengths as 1.3778 and 1.4597 Å, respectively. This difference belongs to the fact that electron density is more delocalized on nitro (NO2) group. Also can be seen from the Table 1, in view of the bond length, most of the calculated parameters are longer than experimental ones and the biggest difference occurs at

C1-N35, with the different values being 0.078 Å when compared with the experimental values [21, 22]. As for the bond angles by comparing the calculated values with experimental ones, the biggest difference is seen in the bond angle of N(34)- C(38)-N(36), with the difference being 6.19° degree. The (p-nitrophenylamino) fragment at C38 is approximately coplanar with heterocyclic ring. The 1,4 diphenyl rings attached to N35 and N36 subtend dihedral angles of -31.259° and 40.821°, respectively, in relation to the plane of the triazole ring.

The above discrepancies may be due to that the theoretical calculations correspond to the isolated molecules in gaseous phase and the experimental results belong to molecules in solid state. The geometry of the solid-state structures is subject to intermolecular forces, such as van der Waals interactions and crystal packing forces, which make most of the experimental bond lengths be shorter than the theoretical ones. Although the differences, calculated geometrical parameters by using DFT/B3LYP/6-311G(d,p) method represent a good approximation and they are the bases for other calculations, such as IR and UV/Vis spectra.

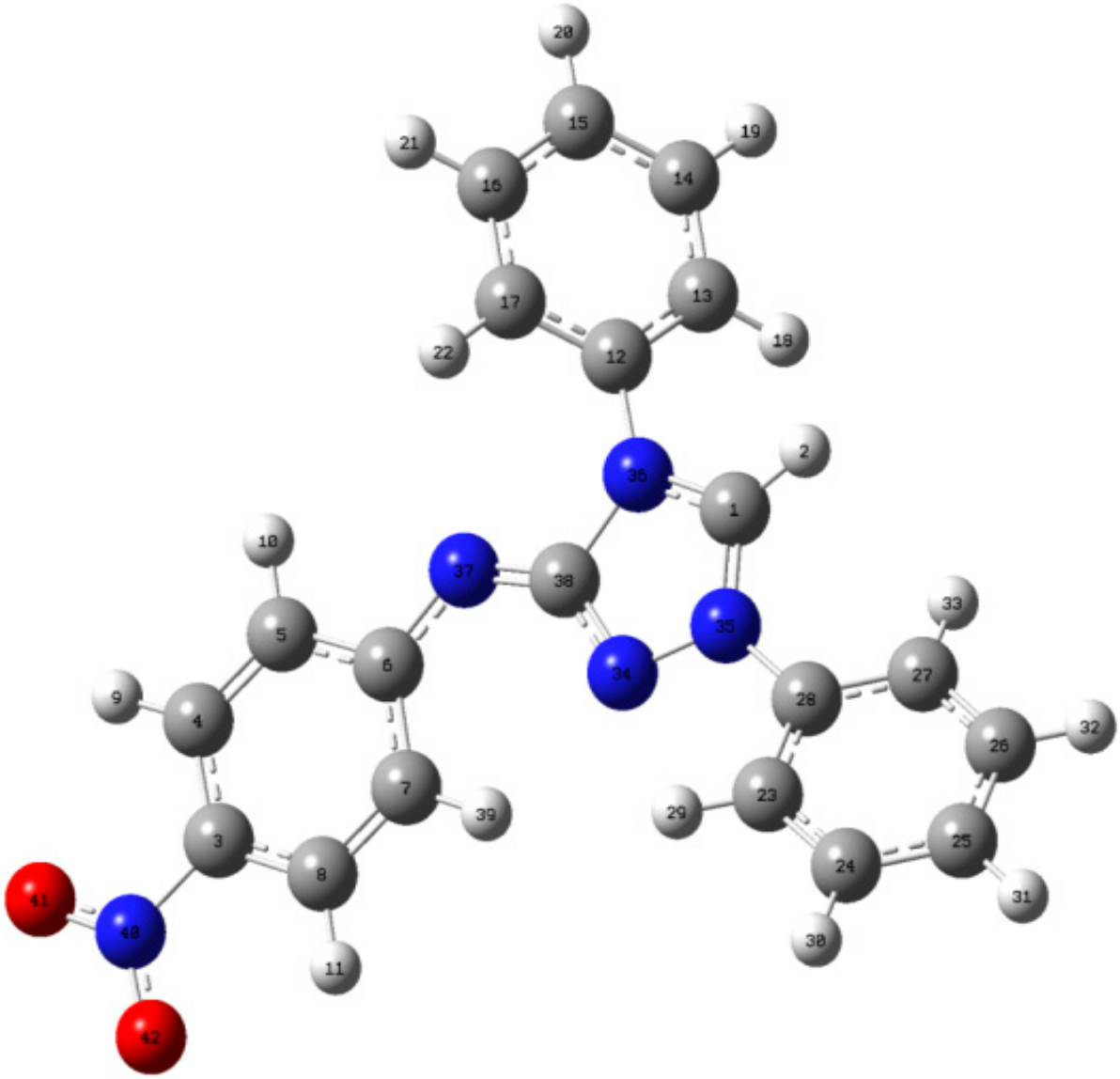

Figure 1. Molecular structure and numbering scheme of Nitronitron

5.2. Vibrational Frequencies

The Nitronitron molecule have 42 atoms and the number of the vibration modes is 140. All fundamental vibrations which possess C_1 symmetry are active in IR spectrum. The observed and calculated vibrational frequencies along with relative intensities, probable assignments at B3LYP/ 6-311G(d,p) level of the title compound are given in Table 2. vibrational frequencies simulated for Nitronitron compound with the unscaled B3LYP/6-311G(d,p) force field are slightly greater than the observed values. These differences can be rectified by scaling the simulated wavenumbers with appropriate factor. It is necessary to scale down the calculated harmonic frequencies to improve the calculated values in agreement with experimental values. The different scale factors can be used for different regions of vibrations to obtain a better agreement between the experimental and computed frequencies. The vibrational frequencies calculated at B3LYP/6-311G(d,p) level were scaled by 0.981 for wave numbers less than 1700 cm^{-1} and 0.976 for higher wave numbers. Figure 3 shows the experimental and the calculated IR spectrum at B3LYP/6-311G(d,p) level of the title compound.

Table 1. Selected Optimized geometrical parameters of Nitronitron compound in the ground state

Parameters	B3LYP/6-311G(d,p)	Exp. [a]	Parameters	B3LYP/6-311G (d,p)	Exp. [a]	Parameters	B3LYP/6-311G(d,p)	Exp. [a]
Bond Lengths (Å)			Bond Angles (^{0})			Dihedral Angles (^{0})		
R(C1,N35)	1.3221	1.400(2)	A(N35,C1,N36)	107.903	103.07	D(N36,C1,N35,N34)	-0.835	-
R(C1,N36)	1.3407	1.411(2)	A(N35,N34,C38)	105.873	104.95	D(N35,N34,C38,N36)	0.234	-
R(N34,N35)	1.3702	1.410(2)	A(C1,N35,N34)	112.230	110.79	D(C1,N35,C28,C27)	-31.259	-
R(N34,C38)	1.3539	1.290(2)	A(C1,N35,C28)	127.161	129.13	D(C1,N36,C12,C13)	40.821	-
R(N35,C28)	1.4264	1.418(2)	A(N34,N35,C28)	120.519	116.30	D(C38,N36,C12,C17)	-137.413	-
R(N36,C38)	1.4476	1.383(2)	A(C1,N36,C38)	106.985	107.04	D(C6,N37,C38,N34)	-2.413	-
R(N36,C12)	1.4276	1.444(2)	A(C1,N36,C12)	124.882	125.66	D(C6,N37,C38,N36)	177.383	-
R(C3,C4)	1.3972	1.377	A(C38,N36,C12)	128.115	122.47	D(C38,N37,C6,C7)	-1.426	-
R(C3,C8)	1.3931	1.377	A(N34,C38,N36)	107.00	113.19	D(C4,C3,C8,C7)	-0.156	-
R(C4,C5)	1.3796	1.378	A(C4,C3,C8)	120.812	119.52	D(C3,C4,C5,C6)	-0.172	-
R(C5,C6)	1.4168	1.391	A(C3,C4,C5)	119.123	120.92	D(C4,C5,C6,C7)	0.395	-
R(C5,H10)	1.0830	0.950	A(C4,C5,C6)	121.798	119.72	D(C5,C6,C7,C8)	-0.267	-
R(C6,C7)	1.4171	1.391	A(C5,C6,C7)	117.534	119.5	D(C6,C7,C8,C3)	-0.077	-
R(C7,C8)	1.3854	1.384	A(C6,C7,C8)	120.801	119.74	D(C17,C12,C13,C14)	1.378	-
R(C12,C13)	1.3963	1.377	A(N36,C12,C13)	119.221	119.97	D(C12,C13,C14,C15)	-0.945	-
R(C12,C17)	1.3954	1.378	A(N36,C12,C17)	120.113	119.13	D(C14,C15,C16,C17)	0.605	-
R(C13,C14)	1.3918	1.377	A(C13,C12,C17)	120.660	120.87	D(C28,C23,C24,C25)	0.183	-
R(C14,C15)	1.3925	1.380	A(C12,C13,C14)	119.645	119.50	D(C24,C23,C28,C27)	0.924	-
R(C15,C16)	1.3939	1.378	A(C14,C15,C16)	119.808	120.42	D(C4,C3,N40,O41)	0.054	-
R(C3,N40)	1.4597	1.50	A(C12,C17,C16)	119.072	119.52	D(C8,C3,N40,O42)	0.206	-
R(C16,C17)	1.3910	1.377	A(C12,C17,H22)	119.486	120.20			
R(C17,H22)	1.0796	0.950	A(C24,C23,C28)	119.010	119.62			
R(C23,C24)	1.3908	1.382	A(C28,C23,H29)	119.181	120.20			
R(C23,C28)	1.3937	1.383	A(C26,C27,C28)	119.215	119.82			
R(C24,C25)	1.3937	1.383	A(C28,C27,H33)	120.659	120.1			
R(C25,C26)	1.3935	1.368	A(N35,C28,C23)	118.771	119.11			
R(C26,C27)	1.3912	1.379	A(N35,C28,C27)	120.147	121.21			
R(C27,C28)	1.3951	1.389	A(C23,C28,C27)	121.081	119.67			
R(N40,O41)	1.2294	1.21	A(C3,N40,O41)	117.991	117.1			
R(N40,O42)	1.2296	1.21	A(C3,N40,O42)	118.095	117.5			
R(C38,N37)	1.2953	-	A(O41,N40,O42)	123.913	125.3			
R(C6,N37)	1.3778	-						

Table 2. Experimental and calculated IR spectral data of Nitronitron together with their assignment

No.	B3LYP/6-311G(d,p)			Experimental	Vibrational assignment
	Wavenumbers(cm^{-1})		IR Intensity	Wavenumbers(cm^{-1})	
	Unscaled	scaled			
1	25	25	0.31	-	Lattice vibration
2	31	30	0.46	-	Lattice vibration
3	32	31	0.18	-	Lattice vibration
4	37	36	0.23	-	Lattice vibration
5	44	43	0.66	-	Lattice vibration
6	54	53	0.26	-	Lattice vibration
7	64	63	0.85	-	Lattice vibration
8	93	91	10.85	-	Lattice vibration
9	96	94	0.71	-	Lattice vibration
10	134	131	3.93	-	Lattice vibration
11	167	164	0.33	-	Lattice vibration
12	197	193	1.76	-	$\gamma\ (CNCN)_{R4}$
13	211	207	0.99	-	Lattice vibration
14	219	215	3.03	-	$\gamma\ (CCC)_{R2,R3} + \gamma\ NCN_{R4}$
15	253	248	1.01	-	$\gamma\ CC_{R2}$-NC
16	288	282	1.94	-	R_1 deformation + $\gamma\ w$ (NO2)
17	298	292	1.78	-	$\gamma\ (CCC)_{R2,R3}$
18	321	315	0.87	-	$\gamma\ (NCH)_{R4} + \gamma\ (C_{R2}$-NC)
19	367	360	2.21	-	$\gamma\ (CCC)_{R3,R1}$
20	389	381	5.17	-	$\gamma\ (CNC)_{R4}$
21	417	409	0.19	-	$\gamma\ (CCC)_{R3}$
22	423	415	4.61	-	$\gamma\ (CCC)_{R1}$
23	425	417	0.21	-	$\gamma\ (CCC)_{R2}$
24	453	444	0.95	-	$\gamma\ (CNC)_{R4}$
25	479	469	12.6	-	$\gamma\ (CCC)_{R1,R3}$
26	508	498	15.47	-	$\beta\ (NO2) + \gamma\ (CCC)_{R1}$
27	519	509	6.4	-	$\gamma\ (CCC)_{R1,R3}$
28	534	523	10.46	-	$\gamma\ (CCC)_{R2}$
29	536	525	0.51	-	$\beta\ (ONC) + \gamma\ (CCC)_{R2}$
30	556	545	11.02	-	$\beta\ (CCC)_{R2} + \gamma\ (CCC)_{R3}$
31	619	607	5.04	-	$\gamma\ (CH)_{R4} + \beta\ (CCC)_{R3}$
32	630	617	0.44	-	$\beta\ (CCC)_{R2}$
33	635	622	5.77	-	$\beta\ (CCC)_{R3}$
34	639	626	3.01	635w	$\beta\ (CCC)_{R1}$
35	665	652	18.46	652 m	$\beta\ (CCC)_{R2}$
36	693	679	22.5	-	$\beta\ (CCC)_{R3} + \gamma\ (NCN)_{R4}$
37	698	684	0.9	-	$\gamma\ (CNNC)_{R4} + \beta\ (CCC)_{R3}$
38	703	689	7.16	691 s	$\gamma\ (CCC)_{R1,R3} + \gamma\ w$ (NO2)
39	706	692	54.03	-	$\gamma\ (CCC)_{R3} + \gamma\ (NCN)_{R4}$
40	709	695	21.88	-	$\gamma\ (CCC)_{R2}$
41	725	711	1.51	-	$\beta\ (CCC)_{R1} + \beta$ (NO2)
42	747	732	29.12	723 m	γ w(NO2)+ $\gamma\ (CH)_{R4}$
43	756	741	17.17	-	$\gamma\ (CH)_{R4,R3}$
44	776	760	28.18	-	$\gamma\ (CH)_{R2}$

Table 2. Continued

45	778	762	48.13	770 vs	$\gamma\ (CH)_{R3,R4}$
46	817	801	6.38	-	$\beta\ (CCC)_{R2}+\beta\ (N\text{-}CN)_{R4}$
47	834	817	5.72	-	$\gamma\ (CH)_{R1}$
48	846	829	0.38	-	$\gamma\ (CH)_{R2}$
49	848	831	1.02	827 w	$\gamma\ (CH)_{R3}$
50	866	849	49.18	843 m	$\gamma\ (CH)_{R1}+\beta\ (NO2)$
51	874	857	58.01	-	$\gamma\ (CH)_{R1}+\beta\ (NO2)$
52	894	876	6.7	872 w	$\gamma\ (CH)_{R2}+\beta\ (CNC)_{R4}$
53	917	899	8.67	-	$\gamma\ (CH)_{R2}$
54	925	907	46.44	-	$\nu\ (CN)_{R4}+\gamma\ (CH)_{R2}$
55	934	915	4.93	920 m	$\gamma\ (CH)_{R3}$
56	975	956	0.06	-	$\gamma\ (CH)_{R2}$
57	980	960	1.49	966 m	$\gamma\ (CH)_{R1}$
58	986	966	0.82	-	$\gamma\ (CH)_{R3}$
59	989	969	0.33	-	$\gamma\ (CH)_{R2}$
60	998	978	2.31	-	$\gamma\ (CH)_{R1}$
61	1011	991	6.11	-	$\gamma\ (CH)_{R3}+\beta\ (CCC)_{R2}$
62	1012	992	2.14	-	$\gamma\ (CH)_{R3}+\beta\ (CCC)_{R2}$
63	1017	997	1.81	-	$\beta\ (CCC)_{R3,R1}$
64	1018	998	3	-	$\beta(CCC)_{R3,R1}+\beta(NCN)_{R4}$
65	1031	1010	1.69	1002 w	$\beta\ \ (CH)_{R1}$
66	1047	1026	17.98	-	$\beta\ \ (CH)_{R3}$
67	1049	1028	0.64	1020 w	$\beta\ (CH)_{R2}$
68	1072	1051	140.04	1061 m	$\nu\ (NN)_{R4}+\beta\ (CH)_{R4}$
69	1104	1082	20.91	-	$\beta\ (CH)_{R2}$
70	1105	1083	2.94	-	$\beta\ (CH)_{R3}$
71	1121	1099	121.74	-	$\nu\ C_{R1}\text{-}NO2$
72	1133	1110	22.41	-	$\beta\ (CH)_{R1}$
73	1161	1138	48.99	-	$\nu\ (CN)_{R4}+\beta\ (CH)_{R1,R2,R3}$
74	1176	1152	1.29	1150 m	$\beta\ (CH)_{R2}$
75	1185	1161	1.44	-	$\beta\ (CH)_{R3}$
76	1197	1173	14.16	-	$\beta\ (CH)_{R3}$
77	1199	1175	8.18	-	$\beta\ (CH)_{R2}$
78	1202	1178	12.94	-	$\beta\ (CH)_{R1}$
79	1236	1211	112.62	-	$\beta\ (CH)_{R4}+\nu\ (N)\text{-}(C)_{R2,R3}$
80	1252	1227	330.12	1229 s	$\nu\ (N)\text{-}(C)_{R1,R3}$
81	1286	1260	12.19	1255 w	$\nu\ (NN)_{R4}+\beta\ (CH)_{R4}$
82	1296	1270	6.06	-	$\nu\ (N)\text{-}(C)_{R2}+\beta\ (CH)_{R1}$
83	1315	1289	1.9	-	$\nu\ (CC)_{R2}+\beta\ (CH)_{R1}$
84	1331	1304	7.83	1285 w	$\beta\ (CH)_{R1}$
85	1345	1318	8.56	-	$\nu\ (CC)_{R3}$
86	1355	1328	3.25	-	$\beta\ (CH)_{R1,R2}$
87	1356	1329	8.5	-	$\nu\ (CC)_{R1}+\beta\ (CH)_{R2,R3}$
88	1357	1330	16.07	-	$\nu\ (CC)_{R1}+\beta\ (CH)_{R2,R3}$
89	1371	1344	812.56	1333 s	$\nu_S\ \ (NO2)$
90	1441	1412	42.23	-	$\nu\ (CC)_{R1}+\nu(N)\text{-}(C)_{R1}$
91	1469	1440	48.13	1425 m	$\nu\ (C\text{-}N)_{R4}+\beta\ (CH)_{R1,R3}$

Table 2. Continued

92	1480	1450	2.36	1454 m	ν $(CC)_{R2}$
93	1497	1467	71.98	-	ν $(CC)_{R3}$
94	1522	1492	88.45	-	ν $(CC)_{R1,R3}$
95	1524	1494	80.61	1491 w	ν $(CC)_{R2}$
96	1533	1502	197.54	1514	ν $(CC)_{R1}$+ ν (N)-$(C)_{R1}$
97	1582	1550	450.71	1537 s	ν $(C=N)R_4$
98	1594	1562	158.29	1570 m	ν_{as} (NO2)+ ν $(CC)_{R1}$
99	1607	1575	22.24	-	ν $(CC)_{R2}$
100	1631	1598	421.64	-	ν $(CC)_{R1,R2,R3}$
101	1637	1604	85.56	1603 s	ν $(CC)_{R3,R1}$
102	1638	1605	27.97	-	ν $(CC)_{R3,R2,R1}$+ν $(C=N)_{R4}$
103	1642	1609	2.49	-	$\nu(CC)_{R3,R2}$
104	1656	1623	69.82	1630 m	ν $(CC)_{R1}$+ ν_{as} (NO2)
105	1695	1661	1116.68	1665 w	ν(N)=($C)_{R4}$
106	3152	3076	8.58	3059 w	ν_{as} $(CH)_{R2}$
107	3160	3084	18.15	-	ν_{as} $(CH)_{R2}$
108	3174	3098	1.32	-	ν_{as} $(CH)_{R3}$
109	3178	3102	37.36	-	ν_{as} $(CH)_{R2}$
110	3182	3106	4.43	-	ν_{as} $(CH)_{R3}$
111	3186	3110	25.58	-	ν_S $(CH)_{R2}$
112	3188	3111	5.72	-	ν $(C_7$- $H_{39})_{R1}$
113	3191	3114	14.9	-	ν_{as} $(CH)_{R3}$
114	3199	3122	11.66	3117 w	ν_S $(CH)_{R3}$
115	3222	3145	1.52	-	ν $(C_{13}$- $H_{18})_{R2}$+ν $(C_{27}$-$H_{33})_{R3}$
116	3223	3146	1.65	-	ν $(C_{13}$- $H_{18})_{R2}$+ν $(C_{27}$-$H_{33})_{R3}$
117	3224	3147	3.12	-	ν_{as} $(CH)_{R1}$
118	3227	3150	2.79	-	ν $(C_7$- H_{39},C_8-$H_{11})_{R1}$
119	3244	3166	5.39	-	ν $(C_4$- H_9,C_5-$H_{10})_{R1}$
120	3297	3218	25.28	3241w	ν(C_1- $H_2)_{R4}$

w-wagging, *ν*-stretching, ν_s- symmetric stretching, ν_{as}- asymmetric stretching, β-in plane bending, γ-out of plane bending, R_1:(C3-C4-C5-C6-C7-C8), R_2:(C12-C13-C14-C15-C16-C17), R_3:(C23-C24-C25-C26-C27-C28), R_4:triazole ring, s-strong, vs-very strong, m-medium, w-weak.

5.2.1. C-H Vibrations

The aromatic compounds shows the appearance of C-H stretching vibrations in the spectral range 3000-3100 cm^{-1} [23]. The observed bands at 3059, 3117 cm^{-1} attributed to C-H stretching vibrations of the title compound. DFT computations predict this mode at 3076, 3122 cm^{-1} for B3LYP/6-311G(d,p) level of theory. The other CH stretching modes (C13-H18, C27-H33, C7-H39, C8-H11, C4-H9, C5-H10, C1-H2) are computed from 3145 to 3218 cm^{-1}. The C-H in-plane bending bands of aromatic compounds are observed in the spectral range 1300-1000 cm^{-1} [24]. The observed bands at 1002, 1020, 1150, 1285 cm^{-1} of title compound can attributed to the C-H in-plane bending vibrations. The respective calculated bands are 1010, 1028, 1152, 1304 cm^{-1} at B3LYP/6-311G(d.p) level for C-H in-plane bending vibrations. The absorption bands arising from C-H out-of-plane bending vibrations are usually observed in the spectral range 1000-750 cm^{-1} [25]. The computed vibrations at 762, 831, 849, 876, 915, 960 cm^{-1} are assigned C-H out-of-plane bending vibrations using B3LYP/6-311G(d,p) which are comparable to experimental data at 770, 827, 843, 872, 920, 966 cm^{-1}. The results showed that the theoretical data nearly coincide with experimental ones and these assignments are in good agreement with literature data [24, 25].

5.2.2. C-C Vibrations

The C=C stretching modes in Benzene rings are in general appear in the spectral range 1650-1400 cm^{-1}[26]. For the title compound the observed C=C stretching vibrations are found at 1454, 1491, 1514 1603, 1630 cm^{-1} and the respective calculated bands are assigned at 1450, 1494, 1502, 1604, 1623 cm^{-1}. The CCC in-plane bending modes of aromatic rings is observed bands at 635, 652 cm^{-1} which is comparable to theoretical data at 626, 652 cm^{-1} and CCCC out-of-plane bending mode is not observed in the spectrum of the title compound. These assignments are in good agreement with B3LYP/6-311G(d,p) method and as well as with the

literature data [27].

5.2.3. C-N,C=N, N-N Vibrations

The recognition of C-N, C=N, and N-N vibrations is a very difficult task, since the mixing of several bands are possible in this region. The observed bands in IR at 1665 cm^{-1} belong to C(aromatic ring) = N stretching vibration, while the calculated value of this band was appeared at 1661 cm^{-1} for the title compound. The observed band at 1425 cm^{-1} can be assigned to the C-N stretching vibration of 1,2,4 triazole ring and the calculated value of the mention mode was found at 1440 cm^{-1}. The C=N stretching mode of triazole ring is observed band at 1537 cm^{-1}, while the calculated value was appeared at 1550 cm^{-1}.

The observed band at 1255 cm^{-1} of title compound can be assigned to the N-N stretching mode and the calculated value of the mentioned mode was appeared at 1260 cm^{-1}. Some of vibrational bands are combined with the other vibrational ones. These assignments are in good agreement with B3LYP/6-311G(d,p) method and as well as with the literature data [28-31].

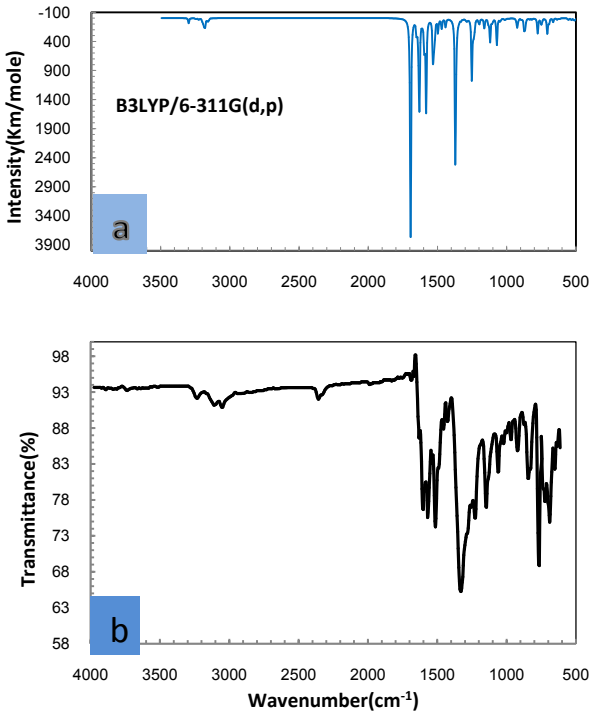

Figure 2. Theoretical (a) and experimental (b) FT-IR spectra of Nitronitron

5.2.4. NO_2 Group

Aromatic Nitro(NO2) group compounds show a very strong asymmetric and strong symmetric stretching vibrations at 1540-1614 cm^{-1} and 1320-1390 cm^{-1}, respectively [32]. The IR spectrum of the Nitronitron two absorption at 1333, 1570 cm^{-1} with strong and medium have been assigned to NO2 symmetric and asymmetric stretching vibrations, respectively. This resembles the calculated vibrations 1344, 1562 cm^{-1} obtained from DFT. Nitro (NO2) group scissoring modes is observed at 843, cm^{-1} combined with other mode and the calculated value of the mention mode was appeared at 849 cm^{-1}. Furthermore, in plane bending (scissors) of nitro group calculated at 711, 857 cm^{-1}. Out of plane bending (wag) modes of nitro group observed at 691 cm^{-1} combined with the other modes and the calculated value of this mode was appeared at 689 cm^{-1}. Finally, stretching vibration between C(aromatic ring) and nitro group calculated at 1099 cm^{-1}.

5.3. ^{1}H NMR Analysis

Chemical shifts are recognized as an imperative part of the information contained in NMR spectra. The NMR experimental and theoretical chemical shifts are used to identify the organic compounds. GIAO (Gauge Independent Atomic Orbital) method exhibits a faster convergence of the calculated properties upon extension of the basis set used compared with other methods. GIAO approach is one of the most common methods for calculating isotropic nuclear magnetic shielding tensors. In GIAO method, the atomic basis functions depend explicitly on the magnetic field. 1H NMR chemical shifts of the Nitronitron compound are calculated with GIAO procedure using DFT/B3LYP/6-311G(d,p) method and using Tetramethylsilane (TMS) as reference. The NMR spectra calculations were performed by using Gaussian 09 package. The experimental and theoretical 1H NMR spectra are shown in Figure 3. The calculated 1H NMR showed a good agreement with experimental results obtained for the new synthesized Nitronitron compound named (1,4-Diphenyl-3-(p-nitrophenylamino)-1,2,4-triazolium hydroxide). The obtained theoretical results were helpful for the detailed assignments of experimental 1H NMR spectra of the studied compound. Quantum chemical calculations were used for a better understanding of the NMR properties as well as for an analysis of the geometrical parameters in this novel compound. The H atom is the smallest of all atoms and mostly localized on the periphery of molecules; therefore their chemical shifts would be more susceptible to intermolecular interactions in the aqueous solutions as compared to that for other heavier atoms.

The proton chemical shift (1H NMR) of organic molecules generally varies greatly with the electronic environment of the proton. Hydrogen attached or nearby electron-withdrawing atom or group can decrease the shielding and move the resonance of attached proton towards to a higher frequency, whereas electron-donating atom or group increases the shielding and moves the resonance towards to a lower frequency [33]. Experimental and theoretical 1H-NMR spectra of Nitronitron, Figure 3, exhibited signals: 2.48-3.55 ppm was assigned to protons of the solvent Dimethylsulfoxide, a multiplet signal in the range 7.669–8.531(calculated at 7.042-7.840) ppm due to ten aromatic protons of phenyl rings 1 and 2, multiplet signal in the range 8.663-8.690(calculated at 8.120-8.279) ppm due to four protons of (p-nitrophenylamino) ring, and singlet signal at 8.775(calculated at 8.663) ppm due to proton of

triazole ring. By comparing 1H NMR spectrum of phenyl rings 1and 2 with (p-nitrophenylamino) ring, it is found that rings 1,2 protons appear at a much lower field. This is because of the strong electron withdrawing ability of the nitro group. As a result, signals due to rings 1,2 protons are recorded at a higher field than those of (p-nitrophenylamino) ring protons. The theoretical ^{1}H NMR chemical shifts showed an acceptable agreement with experimental ones.

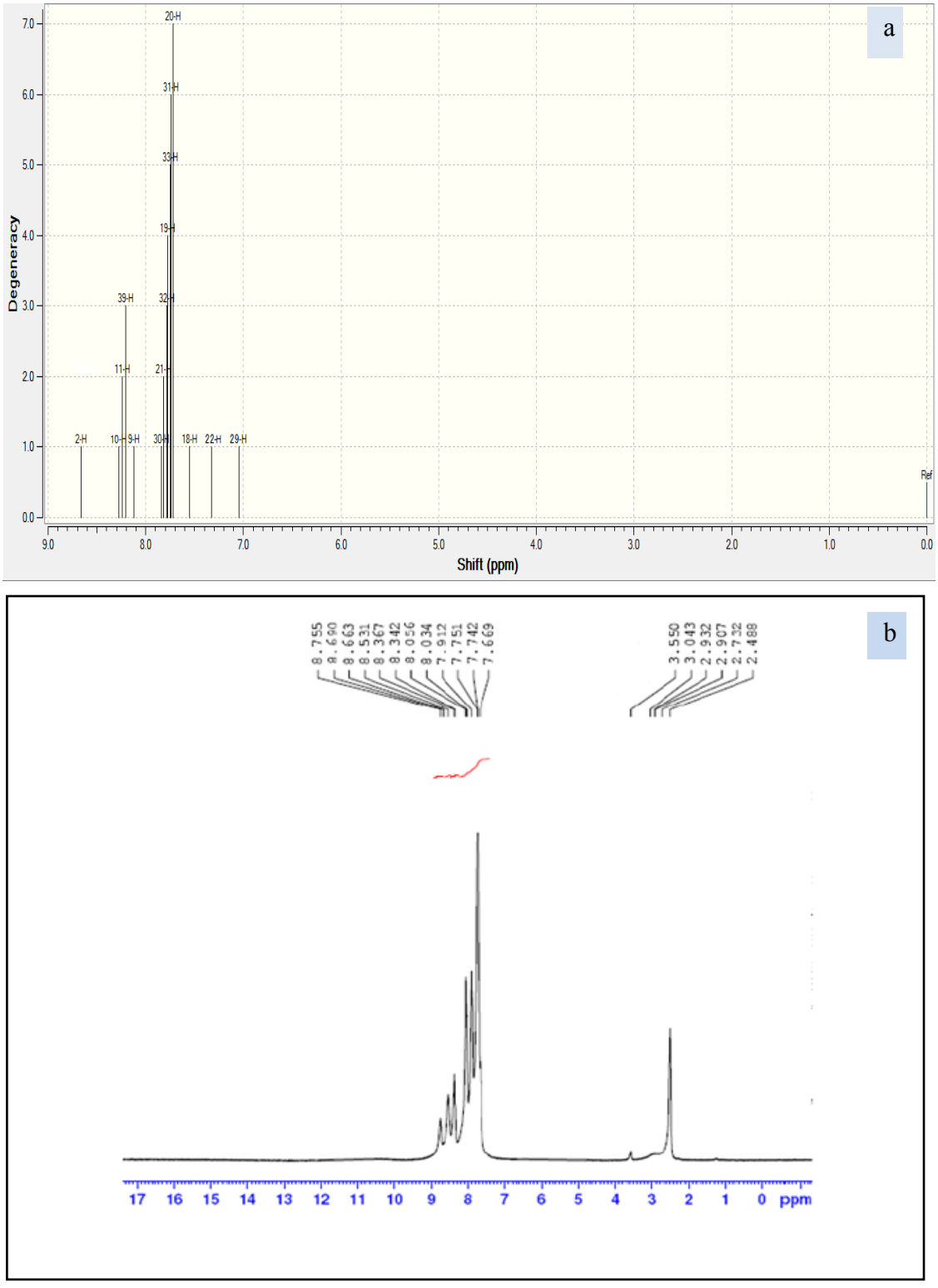

Figure 3. Theoretical (a) and experimental (b) ^{1}H NMR of synthesized compound in DMSO solvent

5.4. HOMO-LUMO Analysis

The frontier molecular orbitals (HOMO and LUMO) are the main orbital participating in chemical reactions and they also used for predicting the most reactive position in π-electron systems. The HOMO energy describes the ability of electron giving, LUMO describes the ability of electron accepting, and the energy gap between HOMO and LUMO describes the molecular chemical stability [34] and it is important parameter in determining molecular electrical transport properties because it is a measure of electron conductivity.

Table 3. The total energy, dipole moment, and frontier molecular orbital energies of Nitronitron obtained by using B3LYP/6-311G(*d,p*)

Property	Nitronitron
Total energy (a.u.)	-1195.52743241
E_{HOMO} (eV)	-5.0151716
E_{LUMO} (eV)	-2.43574612
$\Delta E=E_{LUMO}-E_{HOMO}$ (eV)	2.57942548
Dipole moment (D)	15.0843

In order to investigate the energetic behavior and dipole moment of synthesized compound, optimization were performed. Theoretical calculations included the total energy, HOMO-LUMO energies, energy gap, and dipole moment using B3LYP/6-311G(d,p) level. Results obtained in gas phase are listed in Table 3. and it reveals the energy gap reflect the chemical activity of the molecule. In addition, The energy value of HOMO is computed as (-5.0151716 eV) and LUMO as (-2.43574612 eV), and the energy gap value is (2.57942548 eV) and the dipole moment is (15.0843Debye) in gas phase for the synthesized compound. Lower value in the HOMO and LUMO energy gap explains the eventual charge transfer interactions taking place within the molecule.

The frontier molecular orbital energies were obtained using the B3LYP/6-311G(d,p) level for the optimized molecular structure. A total of 576 molecular orbitals were founded, 93 of which are occupied. The 3D plots of the frontier orbitals; the highest occupied molecular orbital (HOMO) and the lowest unoccupied molecular orbital (LUMO) are shown in Figure 4 that show it is likely to exhibit an efficient electron transfer from 3-(p-nitrophenylamino) group of the HOMO to the 1,4-(diphenyl) group of the LUMO if electronic transitions occur. The HOMO for the computed is localized at the 3-(p-nitrophenylamino) and triazole ring regions, whereas the LUMO is localized at 1,4-(diphenyl) and 1,2,4 triazole regions. This result indicates that the electron transfer from the 3-(p-nitrophenylamino) group to the 1,4-(diphenyl) group through the triazole group. The intramolecular charge transfer (ICT) from HOMO to LUMO occurs through π-conjugated path.

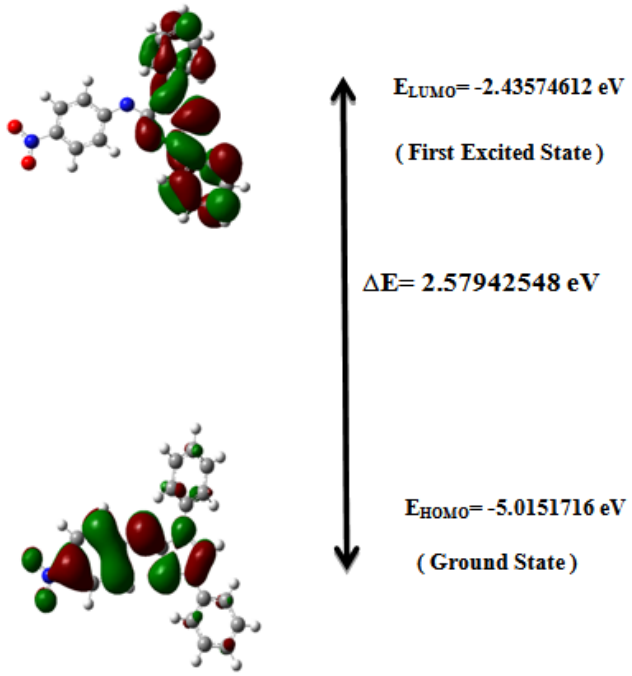

Figure 4. The atomic orbital components of the frontier molecular orbital of Nitronitron

Table 4. The experimental and calculated absorption wavelength (λ), excitation energies and oscillator strengths (*f*) of Nitronitron

Excited states	Experimental	The calculated with TD-DFT/B3LYP/6-311G(d,p) in Vacuum / Solvent (C-PCM)(Chloroform)				Major Contrib.	Transition
	Wavelength(nm)	Wavelength (nm)	Energy (eV)	Osc. Strength	Symmetry		
1	430	495/419	2.50/2.95	0.056/0.476	Singlet-A	HOMO →LUMO 99% / 51%	π-π*
2		374/413	3.31/3.00	0.631/0.0349	Singlet-A	HOMO →LUMO+1 96% / 51%	π-π*
3	340	355/309	3.48/4.01	0.008/0.005	Singlet-A	HOMO →LUMO+2 98% / 97%	π-π*

5.5. UV/Vis Spectrum

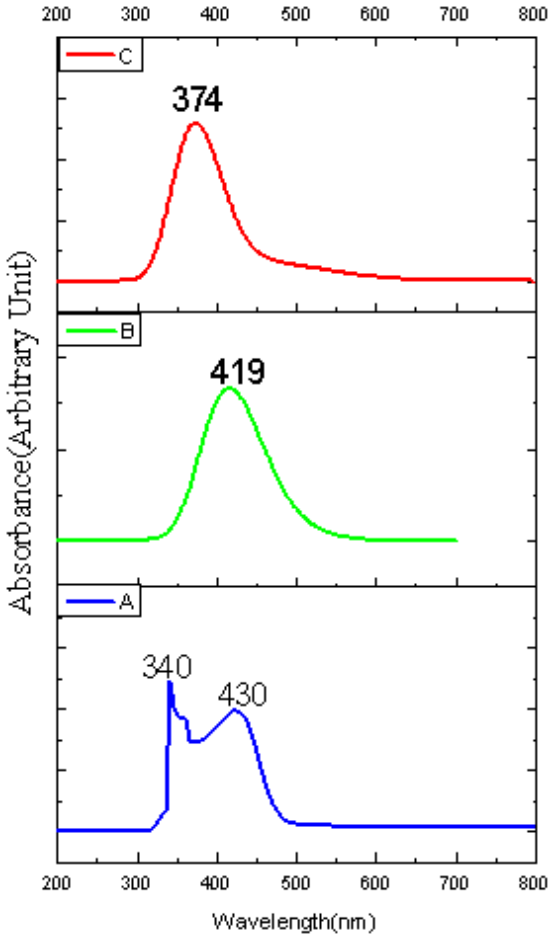

Figure 5. Experimental and calculated UV/Vis spectra of the synthesized compound: (a) Experimental (chloroform solvent), (b) Theoretical in solvent case (chloroform) and (c) in gas phase

UV/Vis spectra have been studied using time dependent - density functional theory (TD-DFT)method based on B3LYP/6-311G(d,p) level optimized structure in order to understand electronic transitions of synthesized compound. The experimental UV/Vis spectrum has been observed in chloroform solvent at room temperature, while the theoretical calculations were performed for gas phase and chloroform solvent. The solvent effect was calculated using the conductor-like polarizable continuum model (CPCM). The experimental and theoretical UV/Vis spectra of the synthesized compound is shown in Figure 5. As seen from Figure 5, in experiment, there exist two bands at 340 and 430 nm, respectively. In theory, there is one brad band and the peak is at 374 nm for gas phase, while for solvent case, there was one broad band has red red-shift with value of 419 nm when comparing with gas phase calculations and can easily be seen that solvent case data is the closest with compared to the experimental absorption bands. The error between the calculated and experimental results is 56 nm for gas phase, and 11 nm for solvent case. These values indicate that the solvent case is more suitable than the gas phase for studying the absorption spectra of the title compound. One of the reasons the difference between the experimental values and the theoretical predictions may be

TD-DFT calculations do not evaluate the spin-orbit splitting; the values are averaged.

For the title compound, the excitation energies, absorption wavelength(λ) and oscillator strength(*f*) of UV/Vis absorption have been calculated in gas phase and chloroform solvent by using TD/DFT/B3LYP method with 6-311G(d,p) basis set are listed in Table 4. The theoretical calculations (solvent case) predict one intense electronic transition at 419 nm with an oscillator strength (f = 0.476), it shows an excellent agreement with the measured experimental value (Exp.= 430 nm) and which corresponds to the electronic transition from HOMO to LIMO with 51% contribution. This transition (HOMO→LUMO) is predicted as π-π* transition.

4. Conclusions

The 1,4-Diphenyl-3-(p-nitrophenylamino)-1, 2,4-triazolium hydroxide (Nitronitron) was synthesized and several properties were studied using experimental techniques and computational chemistry calculations for the first time. The geometry was optimized without any symmetry constraints using DFT/B3LYP method with 6-311G(d,p) basis set. The skeleton of the optimized compound is non-planar. On the same base of optimized geometry, ^{1}H NMR were calculated by using the gauge independent atomic orbital (GIAO)/solvent (DMSO) method and their spectra were simulated and the chemical shifts related to TMS were compared with experimental data, showing an acceptable agreement. The vibrational FT-IR spectrum of compound was recorded and assigned with help of the experimental and computed vibrational wavenumbers. The UV/Vis absorption spectrum was examined in chloroform solvent and compared with the calculated one in gas phase and solvent case using TD-DFT/CPCM approach. The experimental band at 430 nm is attributed mainly to a HOMO-LUMO transition is predicted as π-π* transition. The comparison of the predicted bands was done and shows a good agreement. The calculated HOMO and LUMO energies and energy gap analysis show that the occurring of charge transformation within the molecule. Besides the energies of HOMO and LUMO are negative, which indicate that the synthesized compound is stable.

REFERENCES

[1] Bhimagouda S. Patil, G. Krishnamurthy, N. D. Shashikumar, M. R. Lokesh, and H. S. Bhojya Naik, 2013, "Synthesis and Antimicrobial Activity of Some [1,2,4]-Triazole Derivatives, Journal of Chemistry," Volume 2013, Article, 7 pages.

[2] Ahmet Ozdemir, Zafer Asim Kaplancikli, Gulhan Turan-Zitouni, Mehlika Dilek Altintop, Fatih Demirci, 2011,

"Synthesis of some n-(benzothiazol-2-yl)-2-(4h-[1,2,4]triazol -3- ylsulfanyl) acetamides and their antimicrobial activity," Anadolu University Journal of Science and Technology – C Life Sciences and Biotechnology, 1(2), 145-151.

[3] Bhavin S. Shukla and H. H. Parekh, Synthesis and antimicrobial screening of some thiadiazole derivatives, 9th National Conference on bioactive heterocycles and drug discovery paradigm, ISCB – 2005, Poster- 065.

[4] Stefania F. Barbuceanu, Gabriela L. Almajan, Ioana Saramet, Constantin Draghici, Radu Socoteanu, and Florica Barbuceanu, 2009, New S-alkylated 1,2,4-triazoles incorporating diphenyl sulfone moieties with potential antibacterial activity, J. Serb. Chem. Soc., 74(10), 1041-1049.

[5] R. U. Roy and K. R. DESAI., Synthesis and antibacterial activity of 1, 2, 4-triazoles, 9th National Conference on bioactive heterocycles and drug discovery paradigm, ISCB – 2005, Poster-056.

[6] Xiang-Lin Zhao, Yan-Fang Zhao, Shu-Chun Guo, Hai-Sheng Song, Ding Wang, Ping Gong., 2007, "Synthesis and Anti-tumor Activities of Novel [1,2,4]triazolo [1,5-a] pyrimidines, " molecules, 12(5), 1136-1146.

[7] Korany A. Ali, Eman A. Ragab, Thoray A. Farghalyand Mohamed M. Abdalla, 2011, "Synthesis of new functionalized 3- substituted [1,2,4]triazolo [4,3-a]pyrimidine derivatives: potential antihypertensive agents," Acta Pol. Pharm., 68 (2), 237-247.

[8] M.B. Deshmukh, A.W. Suryavanshi, S.K. Akuskar, P.V. Anbhule, S.R. Dhongade and A.R. Mali, "Synthesis of 5-(1-benzimidazolyl) methyl-4-phenyl-3- substituted mercapto-1, 2,4(4h)-triazoles as antifungal agent," 9th National Conference on bioactive heterocycles and drug discovery paradigm, ISCB – 2005, poster 096.

[9] Ram Janam Singh and Dharmendra Kumar Singh, 2009, "Syntheses of Some 3,5-Diaryl-4H-1,2,4-triazole Derivatives and their Antifungal Activity," E-Journal of Chemistry, 6 (1), 219-224.

[10] Emmanuel N. Nfor, Peter F. Asobo, Justin Nenwa, Oswald N. Nfor, Julius N. Njapba, Romanus N. Njong, and Offiong E. Offiong, "Nickel (II) and Iron (II) Complexes with Azole Derivatives: Synthesis, Crystal Structures and Antifungal Activities," International Journal of Inorganic Chemistry, Volume 2013 (2013), 6 pages, Research Article

[11] Anjali Jha, Y. L. N. Murthy, G. Durga, and T. T. Sundari, 2010, "Microwave-Assisted synthesis of 3,5-Dibenzyl-4-a mino-1,2,4-triazole and its diazo ligand, metal complexes along with anticancer activity," E-Journal of Chemistry , 7 (4), 1571-1577.

[12] Reda M. Abdel-Rahman, Mohammad Saleh I. T. Makki, and Wafa A. Bawazir, 2011, "Synthesis of some more fluorine heterocyclic nitrogen systems derived from sulfa drugs as photochemical probe agents for inhibition of Vitiligo Disease-Part I," E-Journal of Chemistry, 8 (1), 405-414.

[13] Vinod Kumar Pandey, Zehra Tusi, Sumerah Tusi, and Madhawanand Joshi, "Synthesis and biological evaluation of some novel 5-[(3-aralkyl amido/imidoalkyl) phenyl]-1,2,4-triazolo[3,4-b]-1,3,4-thiadiazines as antiviral agents," ISRN Organic Chemistry, Volume 2012 (2012), 7 pages Research Article.

[14] Zucchi, F., Fonsati, M., Trabanelli, G. Proceedings of the 13th International Corrosion Congress; Australian Corrosion Association: Clayton, Australia 1996; Papers 322/1 to 322/9.

[15] El-Agez T.M., El-Tayyan A.A., Abdel-Latif M.S., 2009, "New efficient organic compounds in dye-sensitized solar cells," Journal of the Islamic University of Gaza, 17(1), 61-70.

[16] M.J.T. Frisch, G.W, Schlegel, H.B, Scuseria, G.E, Robb, M.A, Cheeseman, J.R, Scalmani, G, Barone, V, Mennucci, B, Petersson, G.A, Nakatsuji, H, Caricato, M, Hratchian, H.P, Izmaylov, A.F, Bloino, J, Zheng, G, Sonneberg, J L, Hada, M, Ehara, M, Toyota, K, Fukuda, R, Hasegawa, J, Ishida, M, Nakajima, T, Honda, Y, Kitao, O, Nakai, H, Vreven, T, Montgomery, J.A., Jr, Peralta, J.E, Ogliaro, F, Bearpark, M, Heyd, J.J, Brothers, E, Kudin, K.N, Staroverov, V.N, Kobayashi, R, Normand, J, Raghavachari, K, Rendell, A, Burant, J.C, Iyengar, S.S, Tomasi, J, Cossi, M, Rega, N, Millam, J. M, Klene, M, Knox, J.E, Cross, J.B, Bakken, V, Adamo, C, Jaramillo, J, Gomperts, R, Stratmann, R.E, Yazyev, O, Austin, A.J, Cammi, R, Pomelli, C, Ochterski, J.W, Martin, R.L, Morokuma, K, Zakrzewski, V.G, Voth, G.A, Salvador, P, Dannenberg, J.J, Dapprich, S, Daniels, A.D, Farkas, O, Foresman, J.B, Ortiz, J.V, Cioslowski, J, Fox, D.J. Gaussian 09, Revision C. 01, Gaussian, Inc.: Wallinford, CT, 2009.

[17] C. Peng, P.Y. Ayala, H.B. Schlegel, M.J. Frisch, 1996, Using redundant internal coordinates to optimize equilibrium geometries and transition states, J. Comput. Chem. 17 (1), 49-56.

[18] M. Cossi, N. Rega, G. Scalmani, V. Barone, 2003, "Energies, structures, and electronic properties of molecules in solution with C-PCM solvation model," J. Comp. Chem., 24 (6), 669–681.

[19] M.J. Frisch, J.A. Pople, J.S. Binkley, 1984, " Self-Consistent molecular orbital methods25: supplementary function for Gaussian basis sets," J. Chem. Phys., 80 (7), 3265–3269.

[20] R. Ditchfield, "Self-consistent perturbation theory of diamagnetism. I. A Gauge-Invariant LCAO (Linear Combination of Atomic Orbitals) method for NMR chemical shifts," Mol. Phys., 27 (1974) 789–807.

[21] M.A.M. El-Mansy, M.M. El-Nahass, N.M. Khusafan, E.M. El-Menyawy, "DFT approach for FT-IR spectra and HOMO-LUMO energy gap for N-(p-dimethyla minobenzylidene)-p-nitroaniline (DBN)," Spectrochimica Acta Part A: Molecular and Biomolecular Spectroscopy, 111(2013), 217-222.

[22] Biplab Maji, Guillaume Berionni, Herbert Mayr, and Peter Mayer, 5-[(E)-Methoxy(phenyl)methylidene]-1,3,4-triphenyl -4,5-dihydro-1H-1,2,4-triazole, Acta Crystallogr. Sect. E. Struct. Rep. Online, 2012, 68(Pt 12).

[23] R.M. Silverstein, F.X. Webster, Spectroscopic Identification of Organic Compound, sixth ed., John Willey & Sons, New York, 1998.

[24] Arjunan V, Rani T and Mohan S, 201, "Spectroscopic and quantum chemical electronic structure investigations of 2-(trifluoromethyl) aniline and 3-(trifluoromethyl) aniline," J. Mol. Structure, 994(1-3), 179-193.

[25] V. Krishnakumar, N. Prabavathi, 2009, "Analysis of vibrational spectra of 1-chloro-2,4-dinitrobenzene based on density functional theory calculations," Spectrochim. Acta,

72A(4), 738–742.

[26] P.B. Nagabalasubramanian, S. Periandy, S. Mohan, M. Govindarajan, 2009, "FTIR and FT Raman spectra, vibrational assignments, ab initio, DFT and normal coordinate analysis of α,α dichlorotoluene," Spectrochim. Acta, 73A(2), 277-280.

[27] V. Arjunan, R. Santhanam , S. Sakiladevi, M.K. Marchewka, S. Mohan, 2013, "Synthesis and characterization of an anticoagulant 4-hydroxy-1-thiocoumarin by FTIR, FT-Raman, NMR, DFT, NBO and HOMO-LUMO analysis," Journal of Molecular Structure, vol. 1037, 305-316.

[28] Sabir Hussain, Jyoti Sharma and Mohd. Amir, 2008, Synthesis and antimicrobial activities of 1,2,4-triazole and 1,3,4-thiadiazole derivatives of 5-amino-2-hydroxybenzoic acid, E- Journal of Chemistry, 5(4), 963-968.

[29] Halil Gokce, Onur Akyildirim, Semiha Bahceli, Haydar Yuksek, Ozlem Gursoy Kol, 2014, "The 1-acetyl-3-methyl-4-[3-methoxy-4-(4-methylbenzoxy) benzylidenamino]-4,5-dihydro-1H-1,2,4-triazole-5-one molecule investigated by a joint spectroscopic and quantum chemical calculations," Journal of Molecular Structure, vol. 1056-1057, 273-284.

[30] Arti Singh, A K Wahi, 2011, "Synthesis, characterization and Antimicrobial activity of some new Mannich bases derived from 4-amino triazoles," RJPBCS, 2(2), 896-903.

[31] Said A. S. Ghozlan, Salwa F. Mohamed, Abd El-Galil E.Amir, El-Sayed E. Mustafa and Ahmed A. Abd El-Wahab, 2009, "Synthesis and reactions of some new 2,6-Bis-substituted pyridine derivatives as antimicrobial agents," World Journal of Chemistry, 4(1), 83-88.

[32] E.K. Meislich, H. Meislich and J. Sharefkin, 1993, 3000 solved problems in organic chemistry, vol.2, McGraw-Hill, New York.

[33] N. Subramania, N. Sundaraganesan, J. Jayabharathi, 2010, "Molecular structure, spectroscopic (FT-IR, FT-Raman, NMR, UV) studies and first-order molecular hyperpolarizabilities of 1,2-bis(3-methoxy-4-hydroxybenzyli dene) hydrazine by density functional method," Spectrochim. Acta A, 76(2), 259–269.

[34] K. Fukui, 1982, Role of Frontier Orbitals in Chemical Reactions, Science, 218(4574), 747-754.